Korean J. Chem. Eng., 32(11), 2247-2256 (2015)
DOI: 10.1007/s11814-015-0072-4

pISSN: 0256-1115
eISSN: 1975-7220

Removal of Co(II) from aqueous solutions by sulfonated magnetic multi-walled carbon nanotubes

Juanjuan Yang*, Yunhui Dong*,†, Jun Li*, Zhengjie Liu, Fanlian Min*, and Yueyun Li*,†**

*Department of Chemical Engineering, Shandong University of Technology, Zibo 255049, P. R. China
**Institute of Intelligent Machines, Chinese Academy of Sciences, Hefei, Anhui 230031, P. R. China
(*Received 16 October 2014 • accepted 8 April 2015*)

Abstract−Sulfonated magnetic multi-walled carbon nanotubes (SMMWCNTs) were applied in the sorption of Co(II) from aqueous solutions. The SMMWCNTs were prepared and characterized by scanning electron microscope (SEM), Fourier transform infrared (FTIR), and X-ray diffractometer (XRD) test. A large number of influencing factors to the sorption process were investigated, such as pH, ionic strength, contact time, cations, anions, humic acid (HA), fulvic acid (FA) and temperature. The results indicated that the Co(II) sorption was strongly controlled by the pH and ionic strength. Moreover, foreign anions, such as F^-, Cl^- and Br^-, had an obvious effect on the sorption process, which depended on the electronegativity of the anions. On the other hand, cations restrained sorption strongly, such as Mg^{2+} and Ca^{2+}. The existence of HA/FA enhanced sorption process at pH<8 while weakened at pH>8. As revealed by the sorption results, the Langmuir adsorption model was more favorable than the Freundlich adsorption model, and the pseudo-second-order model could fit the data much better than the pseudo-first-order. The thermodynamic analysis suggested that sorption was spontaneous and endothermic. What's more, the stability experiments of the SMMWCNTs showed that SMMWCNTs could maintain excellent magnetic stability and dispersion stability. Thus, this SMMWCNTs sorbent was believed to be a promising material for the selective removal of Co(II) from heavy metal-containing wastewater.

Keywords: Co(II), Sorption, Sulfonated Magnetic Multi-walled Carbon Nnanotubes

INTRODUCTION

Industrial wastewater, especially metal-containing effluent, has been threatening human health as a global focus in recent decades. The superfluous accumulation of heavy metal has destroyed the ecological equilibrium [1,2]. As one of the common heavy metals, cobalt is a trace element in the human body present in vitamin B12 [3] and enzymes [4]. Nevertheless, it can result in nausea [5], lung irritation [6] and reproductive problems [7] with excess amount. Therefore, the removal of cobalt from different effluents is quite important to environment protection. There have been some methods for the removal of Co(II) and other heavy metal from wastewater, such as coagulation [8], electrochemical treatment [9], sorption [10-12], membrane separation [13] and ion exchange [14]. Among them, sorption is considered as one of the potential methods with low cost, simplicity and convenience. Different adsorbents have been reported for the removal of Co(II) and other heavy metal from aqueous solution such as activated carbon [15], carbon nanotubes [16], graphene [2,17], bentonite [18], and other adsorbents [19-24]. Activated carbon fiber is widely applied for adsorption because the speed of intra-particle adsorption is faster than activated carbon in powdered and granular forms [25]. Researchers have been focusing on developing novel adsorbents bearing large sorption capacity and sufficient suitability.

Owing to the large specific surface areas and unique morphologies, multi-walled carbon nanotubes (MWCNTs) have attracted attention for wastewater treatment since being developed by Iijima in 1991 [26]. Carbon nanotube composites have been considered to be a prominent adsorbent [27,28]. Sankararamakrishnan et al. synthesized composite nanofloral clusters with carbon nanotubes and activated alumina for the first time, which exhibited a high performance for the removal of Cd(II) and Cr(VI) [29]. Some researchers successfully synthesized adsorptive membrane of ceramic/carbon nanotubes composite and proved that membrane had good adsorption capacity for copper removal [30].

Because of high cost and difficult separation from solutions, the application of MWCNTs is limited. For full performance, MWCNTs are coated by Fe_3O_4 for magnetic separation. Xu et al. reviewed the MWCNTs/magnetite composite for wastewater treatment and photocatalytic technology as nanosorbents or photocatalysts [31].

However, it is also difficult to scale up the MWCNTs because they are easily aggregated in aqueous solutions. Therefore, how to disperse MWCNTs is the key to fully display sorption performance. Mubarak et al. reported that modifying the surface of MWCNTs can improve their dispersion performance [32]. From this point of view, we expected that incorporating hydrophilic group ($-SO_3H$) onto the surface of MWCNTs might overcome the aggregation and dispersion problem of MWCNTs.

In this paper, sulfonated magnetic multi-walled carbon nanotubes were modified with concentrated sulfuric acid to introduce

†To whom correspondence should be addressed.
E-mail: dyh651118@126.com, liyueyun71@163.com

hydrophilic -HSO_3 to MWCNTs. SMMWCNTs were used to study the sorption behaviors of Co(II) from waste water. To evaluate the sorption abilities of SMMWCNTs in removing Co(II) from aqueous solution, we investigated various parameters such as contact time, solution pH and initial Co(II) concentration in the sorption process. In addition, kinetic and thermodynamic studies (ΔG^0, ΔH^0, ΔS^0) were also performed.

EXPERIMENTAL

1. Reagents and Materials

MWCNTs with main range of diameter 10-20 nm and length <2 μm were supplied by Shenzhen Nanotech Port Co., Ltd. The specific surface area of MWCNTs is 100-120 m^2/g according to the manufacturer. Cobalt dichloride was supplied by Jinan chemical reagent factory. Stock solution of Co(II) was prepared by dissolving cobalt dichloride in double distilled water. Ferric chloride hexahydrate was supplied by Tianjin Damao Chemical Reagent Factory. The other desired concentrations of solutions were obtained by diluting the stock solution in appropriate proportions. All chemicals used in this study were analytical reagent grade and used without any further purification.

2. Preparation of SMMWCNTs

SMMWCNTs were synthesized in three steps as shown in Fig. 1. The sulfonated MWCNTs were carried out according to the method described by Farbod [33] and Ge [34]. In brief, the MWCNTs were purified and oxidized by the mixture of sulfuric acid and nitric acid. Then 300 mL 98% H_2SO_4 and 300 mg purified MWCNTs were added to a flask and ultrasonication for 30 min. The above suspension was reacted at 200 °C for 10 h under continuous stirring. H_2SO_4 reacts with hydroxy and other active sites at the surface of oxidized MWCNTs and formed sulfonated MWCNTs. The sample was cooled, filtered, washed and dried in an oven, and then the sulfonated MWCNTs were obtained.

Sulfonated MWCNTs were transferred to a flask with a separatory funnel. Before the addition of sodium hydroxide solution through the separatory funnel, the flask was put on a vacuum pump to keep the vacuum at −0.1 MPa for 30 min. Then the pressure was freed, and NaOH solution was slowly injected into the filter flask. Spontaneously, sulfonated MWCNTs were soaked in the sodium hydroxide solution. After being immersed for 6 h, the solution was transferred to 80±1 °C water bath and afterwards ferric chloride (0.8 g) and diluted hydrazine hydrate (HHA) solution were slowly added and stirred for 1 h. The warm solution was filtered, washed with distilled water and finally dried in a vacuum oven.

3. Characterization

The morphology of the SMMWCNTs samples was characterized by a field emission scanning electron microscope (SEM, *Sirion 200, FEI America*). The Fourier transform infrared (FTIR, *Nicolet 5700, America*) used KBr pellets, the spectral resolution was set to 1 cm^{-1}, and 150 scans were collected for every spectrum. The crystal structure of synthesized materials was determined by an X-ray diffractometer (XRD, *D8 ADVANCE, Germany*). The surface area measurement was carried at −196 °C using an ASAP 2020 system (Micromeritics USA). The SMMWCNTs were degassed for 480 min at 350 °C before sorption measurements. From the N_2 sorption isotherm, the surface area and average pore diameter were calculated by Brunauer-Emmett-Teller (BET) and Barrett-Joyner-Halenda (BJH), respectively, within a relative pressure of 0.05-0.33.

4. Stability Experiments

To assess the stability of SMMWCNTs, the leaching of Fe ions from SMMWCNTs at different pH value was studied. SMMWCNTs were added to aqueous solutions whose pH was adjusted from 2 to 12 and shaken on a shaker. After the separation of solid from liquid phases, the leached Fe concentration was determined by using a spectrophotometer at 508 nm.

5. Sorption Experiments

Batch sorption experiments were carried out in 10 mL polyethylene centrifuge tubes. The suspensions of SMMWCNTs and electrolyte solutions (such as NaCl, $NaClO_4$, KCl, $NaNO_3$) were pre-equilibrated for 24 h and then Co(II) solutions at concentrations between 0.5 and 20 mg/L were added. The pH was adjusted to 2-12 by the addition of HCl or NaOH solutions (0.1 mol/L or 1.0 mol/L). After the solutions were shaken for a certain time, the liquid and solid phases were magnetically separated. The Co(II) concentration of the solutions was measured by spectrophotometry. Sodium acetate acetic acid buffer solution (pH=5.5) and xylenol orange solution were added to the above separated solution of Co(II). After being diluted to the desired concentration, the solution was placed in 50±5 °C water bath for 10 min, then taken out to cool down. The absorbance of the solution was measured at 578 nm. The distribution coefficient (K_d), sorption percentage (%) and sorption capacity at equilibrium (q_e) were calculated by the following equations:

$$K_d = \frac{c_o - c_e}{c_e} \cdot \frac{V}{m} \quad (1)$$

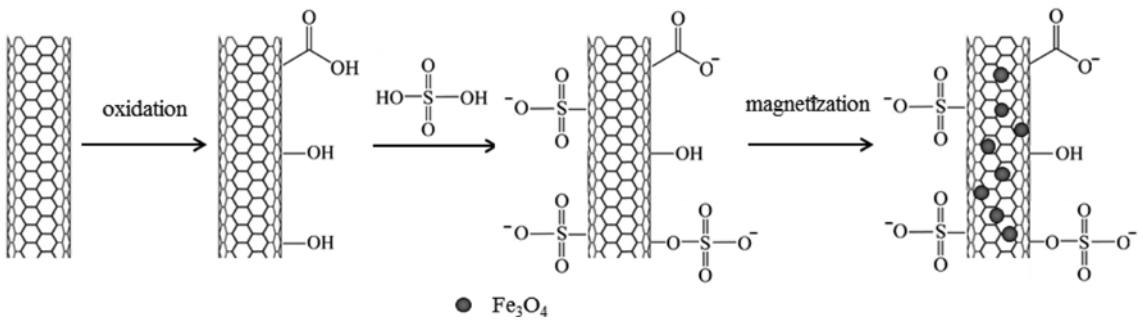

Fig. 1. Synthesis schematic illustration of SMMWCNTs.

$$\text{Sorption}\ (\%) = \frac{c_o - c_e}{c_o} \times 100\% \quad (2)$$

$$q_e = \frac{(c_o - c_e)V}{m} \quad (3)$$

where c_o and c_e are the initial and equilibrium concentrations of Co(II) in the solution (mg/L). V (mL) is the volume of the solution and m (g) is the mass of adsorbents in suspension. All tests were conducted in triplicate to ensure the repeatability of the results.

6. Regeneration Experiments

A regeneration study was also done. After the first adsorption experiment, half of the supernatant was taken out and an equal volume of background electrolyte solution with the same pH value was added. Then the mixture was shaken and magnetically separated under the same experiments conditions as in the previous sorption experiments.

RESULTS AND DISCUSSION

1. Characterization of SMMWCNTs

Fig. 2 displays the typical SEM images of MWCNTs and SMMWCNTs. It is observed that MWCNTs (Fig. 2(A) and (B)) were tubular structure with entangled reticulation. By contrast, SMMWCNTs with different morphology are shown in Fig. 2(C) and (D), which indicates that iron oxide are successfully coated on the surface of MWCNTs.

Fig. 3 shows the Fourier transform infrared (FTIR) spectra of SMMWCNTs and MWCNTs. The peaks at 3,353 cm^{-1} and 3,444 cm^{-1} are assigned to the stretching vibration of hydroxyl [35-37]. The sorption at 2,921 cm^{-1} and 2,892 cm^{-1} are attributed to the symmetric and asymmetric stretching vibration of methylene. The sorption at 1,571 cm^{-1} is attributed to the stretching vibration of C=O of the MWCNTs [38,39]. There are some absorption peaks only observed from SMMWCNTs: the peaks at 580 cm^{-1} and 464 cm^{-1} are due to vibration of Fe-O-Fe in Fe_3O_4 and C-Fe, respectively [40,41], indicating the existence of Fe_3O_4. The band at 1,089 cm^{-1} and 1,047 cm^{-1} may be attributed to the symmetric and asymmetric stretching mode of O=S=O of SMMWCNTs; the peaks at 848 cm^{-1} and 761 cm^{-1} are assigned to S=O band [42], which suggests that the -SO_3H groups are successfully introduced on MWCNTs. In addition, some researchers reported that the existence of oxygen-containing functional groups on MWCNTs provided active sites which were beneficial for the growth of magnetic particles [43,44].

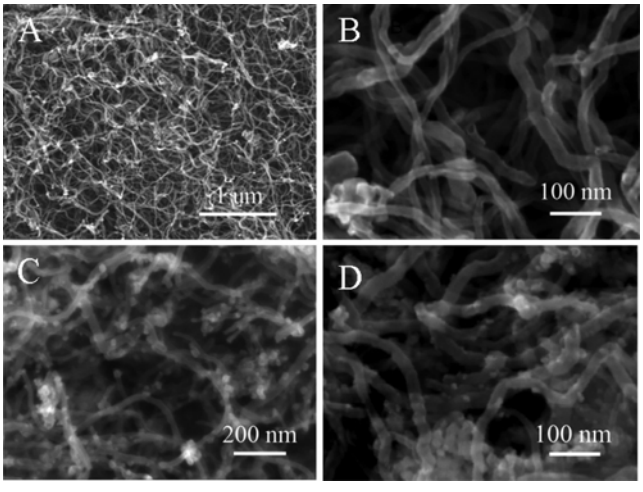

Fig. 2. SEM images of MWCNTs (A), (B) and SMMWCNTs (C), (D).

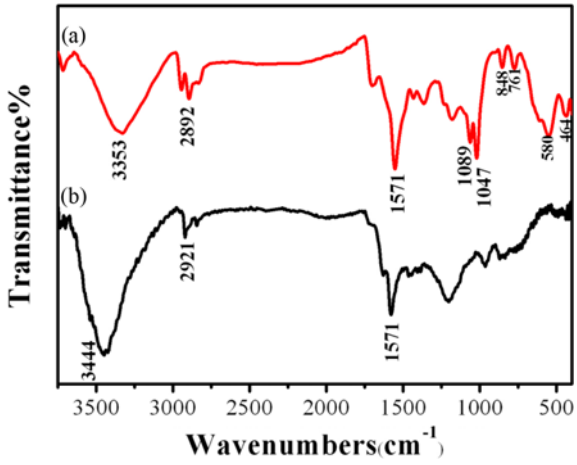

Fig. 3. FTIR spectra of SMMWCNTs (a) and MWCNTs (b).

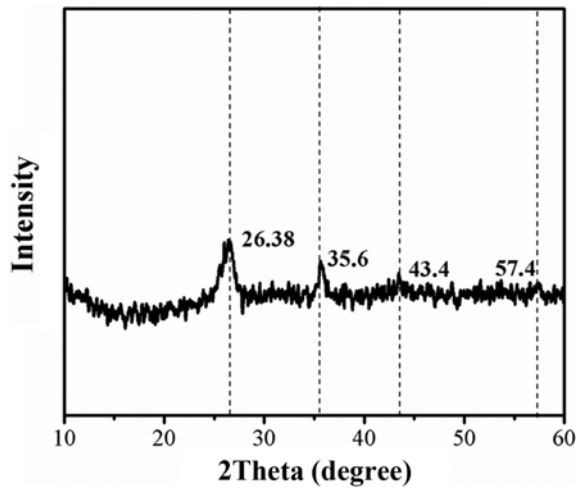

Fig. 4. XRD patterns of SMMWCNTs.

Fig. 4 shows the X-ray diffractometer (XRD) patterns of SMMWCNTs. The diffraction peak at 2θ=26.3° can be indexed as the 002 plane of MWCNTs [45]. The typical peaks of Fe_3O_4 at 35.6°, 43.4° and 57.4° are observed, confirming that iron oxide have been loaded on MWCNTs [46].

The sorption isotherm (a) and pore size distribution curve (b) of the SMMWCNTs are displayed in Fig. 5. The BET surface area of SMMWCNTs is 176.78 m^2/g. As can be seen from 5(a), the relative pressure (P/P_0=0.46-1) indicated the existence of mesopores. When the relative pressure was close to 1.0, a quick increasing of adsorbed N_2 implied that there were a great many of large-mesopores or macropores with size ranging from 20 to 65 nm, which resulted from the opened nanotubes. These results reveal that

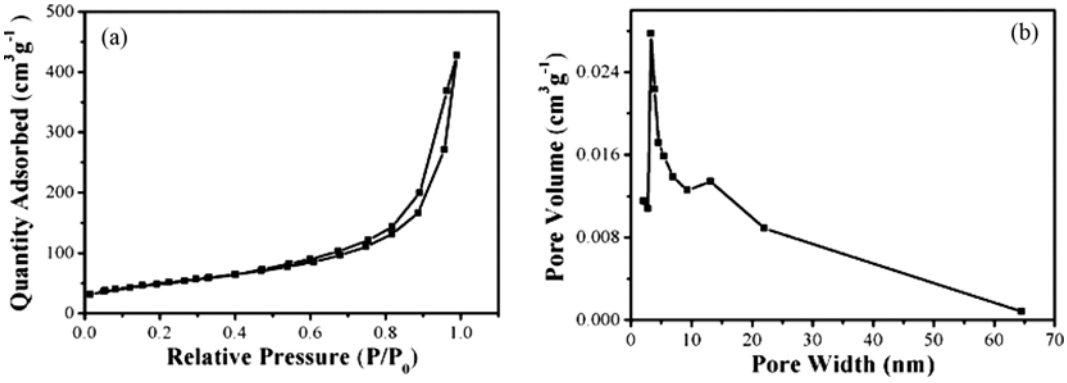

Fig. 5. N_2 sorption isotherm (a); Pore size distribution derived from the nonlocal density functional theory model of the SMMWCNTs (b).

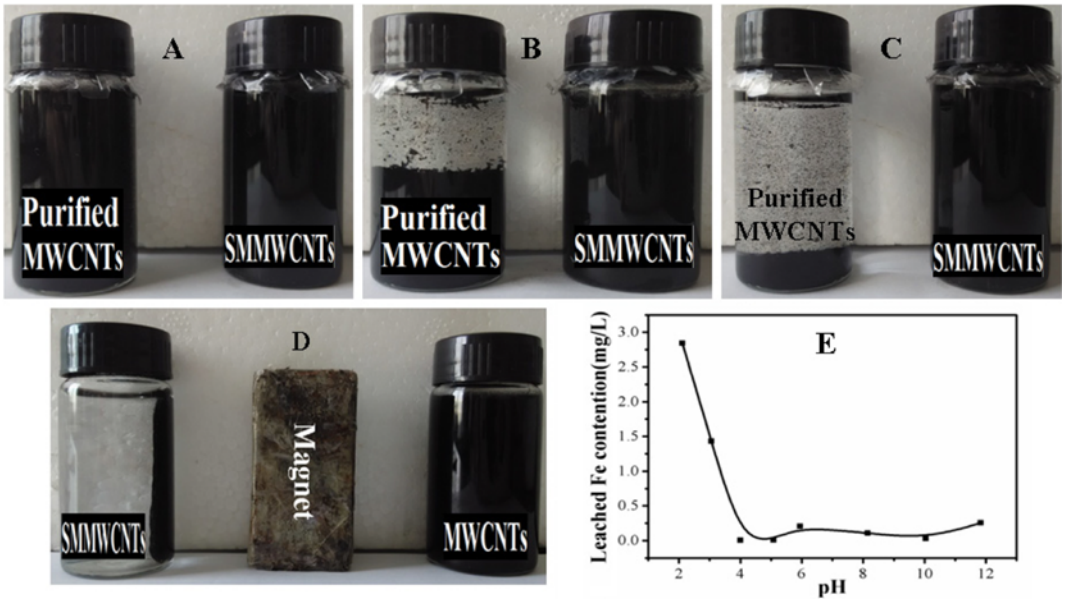

Fig. 6. Photographs of dispersion stability of purified MWCNTs and SMMWCNTs in 0 min (A); 1 min (B); and 12 h (C); MWCNTs and SMMWCNTs response to Magnet (D); Leached Fe content of SMMWCNTs under different pH values (E).

SMMWCNTs are highly porous, which is the foundation of high sorption of Co(II).

2. The Magnetic Stability and Dispersion Stability of the Adsorbent

Fig. 6 shows the dispersion stability of MWCNTs and SMMWCNTs in water. From the digital photos A, B and C, MWCNTs appear as a severe self-aggregation and subsidence in 1 min, while SMMWCNTs can maintain better dispersion stability for 12 hours than MWCNTs. It indicates that SMMWCNTs improve the dispersion stability in the water dramatically. As illustrated in 6D, SMMWCNTs also possess excellent magnetic property.

Fig. 6E shows the concentrations of leaching Fe under different pH levels. The amount of leaching Fe is 2.84 mg/L at pH<4, but almost no leaching Fe appears at pH>4. Intriguingly, SMMWCNTs can maintain good stability in most of the solution pH.

3. Comparative Adsorption of Co(II) by MWCNTs and SMMWCNTs

Fig. 7 shows the sorption isotherms of Co(II) on MWCNTs and

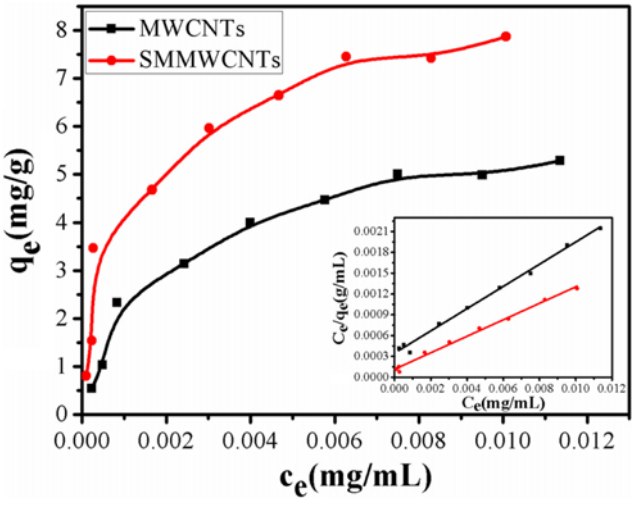

Fig. 7. Sorption isotherms of Co(II) on MWCNTs and SMMWCNTs at 298.15 K (pH=6.0±0.1, m/V=0.3 g/L, I=0.01 mol/L NaCl).

Table 1. Parameters of Langmuir isotherms at different adsorbents

Adsorbent	Langmuir		
	q_{emax} (mg/g)	b (mL/mg)	R^2
MWCNTs	6.244	460	0.996
SMMWCNTs	8.420	1024	0.993

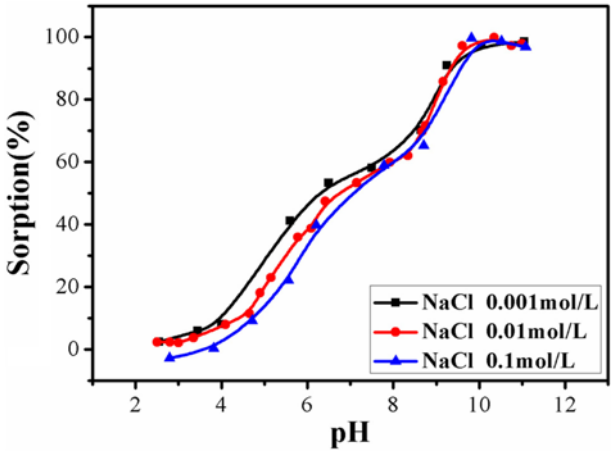

Fig. 8. Effect of pH on the sorption of Co(II) on SMMWCNTs (T= 298.15 K, m/V=0.3 g/L, $C_{[Co(II)]initial}$=0.01 g/L).

SMMWCNTs with the corresponding Langmuir model in additional small figure and the relative parameters calculated from the Langmuir equation in Table 1. One can find that the maximum sorption capacity of SMMWCNTs is higher than that of MWCNTs. This may be due to -SO_3H groups on SMMWCNTs, which could reduce the aggregation of MWCNTs, enhance its dispersion in water, and finally increase sorption capacity.

4. Effect of pH and Ionic Strength

The effect of pH on the sorption of Co(II) to SMMWCNTs is illustrated in Fig. 8. It is observed that the sorption curves are intimately dependent on solution pH. The sorption percentage maintains low value at pH<4, and increases with the increasing of pH, and then reaches the maximum at pH>10. At low pH values, the electrostatic repulsion between the positive charged adsorbent (protonation) and Co(II) leads to a very low sorption. With the pH rising, the electrostatic force between Co(II) and adsorbent has transformed from electrostatic repulsion to electrostatic attraction, and sorption percentage increased gradually. The high sorption percentage at pH>10 can be due to the precipitation of Co(II) on the surface of SMMWCNTs.

Fig. 8 also shows the effect of ionic strength on the sorption of Co(II) on SMMWCNTs in NaCl solutions (0.1 mol/L, 0.01 mol/L, 0.001 mol/L). As can be seen from Fig. 8, the ionic strength influences the Co(II) sorption on SMMWCNTs at pH<10, while no obvious difference is observed at pH>10. The sorption percentage with 0.001 mol/L NaCl is the highest and 0.1 mol/L NaCl is the lowest, which can be explained by ion exchange. The high concentration of NaCl solutions inhibits the adsorption by competing with the adsorption of Co(II) via ion exchange. The result indicates that sorption process is mainly influenced by outer complexation at low pH values.

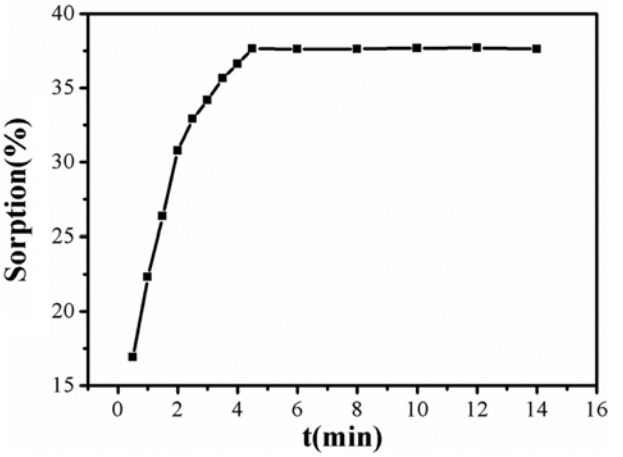

Fig. 9. Effect of contact time on the sorption of Co(II) on SMMWCNTs (T=298.15 K, pH=6.0±0.1, m/V=0.3 g/L, $C_{[Co(II)]initial}$=0.01 g/L, I=0.01 mol/L NaCl).

5. Effect of Contact Time and Kinetic Study

The effect of contact time on the sorption of Co(II) on SMMWCNTs was studied. As can be seen from Fig. 9, the sorption is quite quick and the sorption equilibrium can be achieved in 10 min. The sorption process of Co(II) onto the adsorbent can be divided into three steps. The first step is a fast sorption process, in which Co(II) diffuses and adheres to the external surface of adsorbent. In the second step, Co(II) penetrates into the internal surface of the adsorbent. The third step is diffusion of Co(II) to the sorption site, which is a slow process. According to Cheung's research [47], intraparticle diffusion was the rate-controlling step. To finish these two steps completely, the contact time was set for 24 hours.

A further study on sorption process was conducted via pseudo-first-order (Eq. (4)) and pseudo-second-order (Eq. (5)) kinetic models. Equations are expressed as follows:

$$\ln(q_e - q_t) = \ln q_e - k_1 t \quad (4)$$

$$\frac{t}{q_t} = \frac{1}{k_2 q_e^2} + \frac{t}{q_e} \quad (5)$$

where q_t is the amount of Co(II) adsorbed on adsorbent at time t (min); k_1 and k_2 are rate constant of pseudo-first-order and pseudo-second-order kinetics respectively.

Fig. 10 represents the linear plots of data shown in Table 2 based on the pseudo-first-order and pseudo-second-order kinetic models. Among them, Fig. 10(b) shows good linearity. In addition, the correlation coefficient (R^2) for pseudo-second-order is very close to 1. Hence, this sorption process can be defined as pseudo-second-order kinetic model.

6. Effect of Cations

Fig. 11(a) shows the effect of divalent cations on the removal of Co(II) from aqueous solutions. From Fig. 11(a), the presence of Ca^{2+} and Mg^{2+} decreases the Co(II) sorption percentage at 3<pH<8 and no obvious difference is observed at pH>8. The reason for no obvious difference at pH>8 is that Co(II) begin to precipitate whichever background cations are mixed in solution. The decrease at pH>

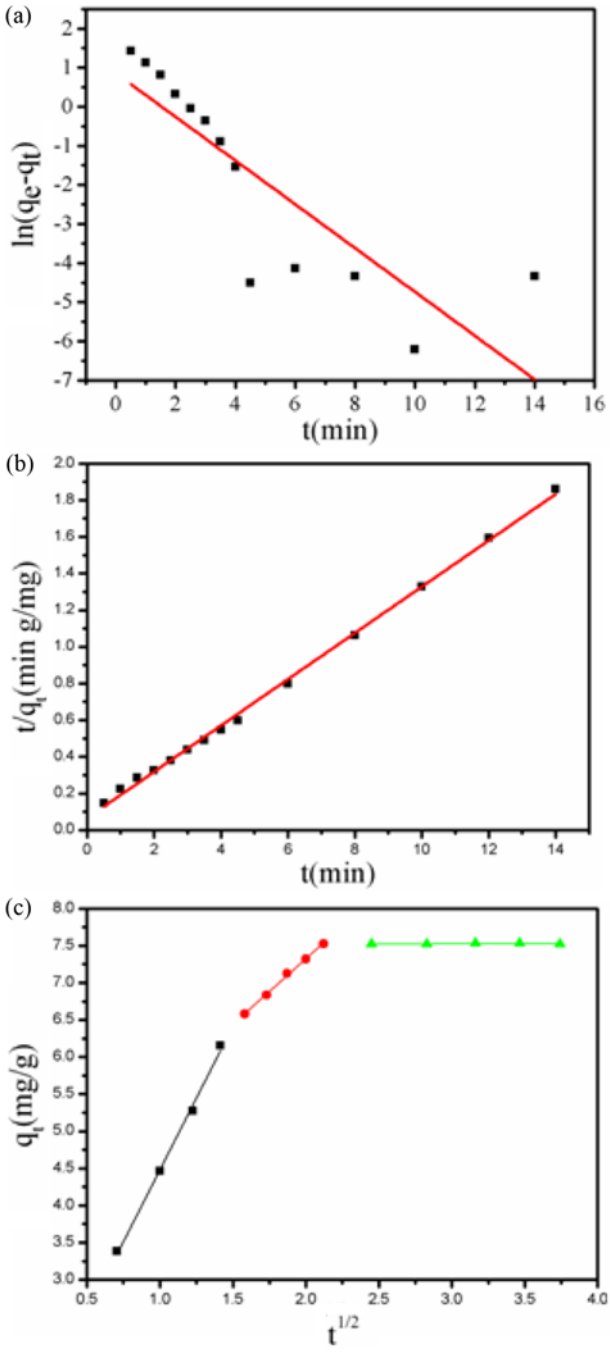

Fig. 10. Plot of pseudo-first-order kinetic models (a); pseudo-second-order kinetic models (b); intraparticle diffusion model (c) for the adsorption of Co(II) on SMMWCNTs (T=298.15 K, pH=6.0±0.1, m/V=0.3 g/L, $C_{[Co(II)]initial}$=0.01 g/L, I=0.01 mol/L NaCl).

Table 2. Kinetic model parameters for the adsorption of Co(II) on SMMWCNTs

C_0 (mg/mL)	Pseudo-first-order kinetic model			Pseudo-second-order kinetic model		
	q_e (mg/g)	k_1	R^2	q_e (mg/g)	k_2	R^2
0.01	2.362	0.560	0.688	7. 937	0.252	0.998

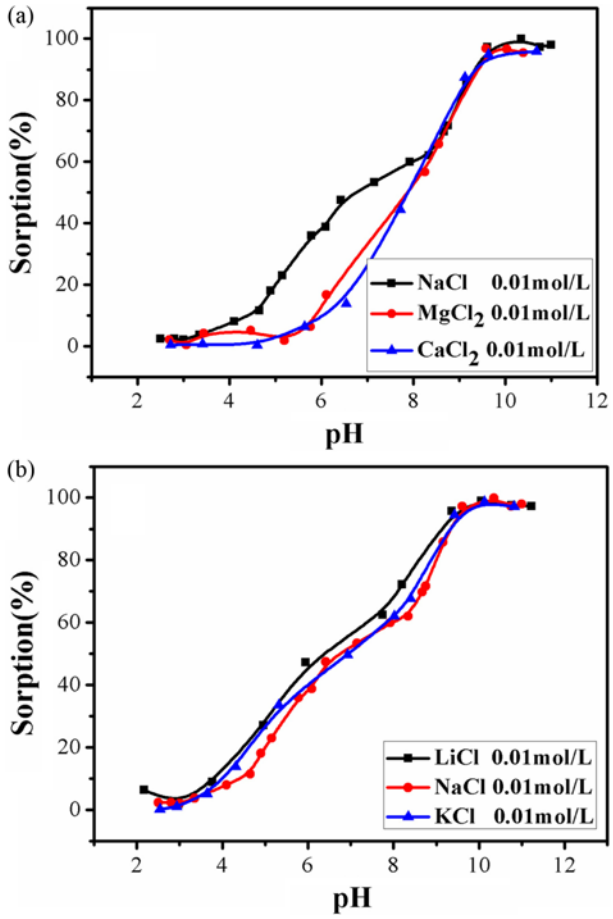

Fig. 11. The effect of different cations on the sorption of Co(II) on SMMWCNTs (T=298.15 K, m/V=0.3 g/L, $C_{[Co(II)]initial}$=0.01 g/L).

8 can be interpreted by the competition between divalent cations and Co(II) to combine with the surface functional groups on SMMWCNTs. A previous study reported that cations sorption percentage decreased with the increasing of competition ion valence [48]. Herein, divalent cations are more likely to be adsorbed on the surface of SMMWCNTs at 3<pH<8 and thereby reduce Co(II) sorption on SMMWCNTs.

Fig. 11(b) shows the effect of monovalent cations on the sorption of Co(II) on adsorbent. One can see that foreign monovalent cations have no influence on the sorption of Co(II) on adsorbent. Radius order of hydrations is Na^+ (2.76A)<K^+ (2.32A)<Li^+ (3.4A) [49]. These positively charged monovalent cations may form complexes or precipitation due to the functional group on the surface of SMMWCNTs. But the results indicate that the sorption of Co(II) on SMMWCNTs is not influenced by Na^+, K^+ and Li^+ obviously, and it can be explained that the complexation occurs only on the surface of SMMWCNTs. Thus the influence of Na^+, K^+ and Li^+ on the sorption of Co(II) can be ignored. This result is similar to Cu(II) sorption on loofah fibers [19].

7. Effect of Anions

Fig. 12(a) and (b) clearly show the effect of different monovalent anions on the sorption of Co(II). From Fig. 12(a), sorption

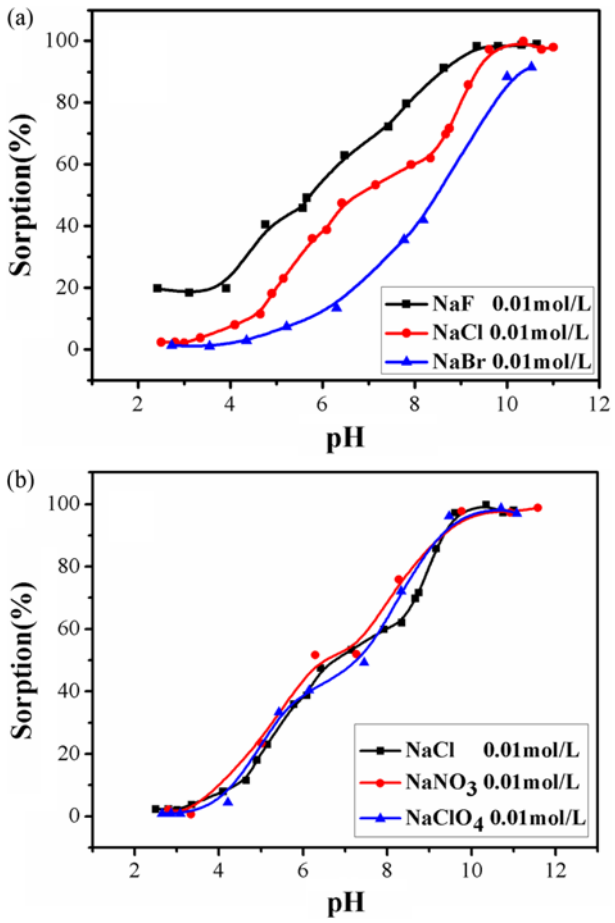

Fig. 12. The effect of different anions on the sorption of Co(II) on SMMWCNTs (T=298.15 K, m/V=0.3 g/L, $C_{[Co(II)]initial}$=0.01 g/L).

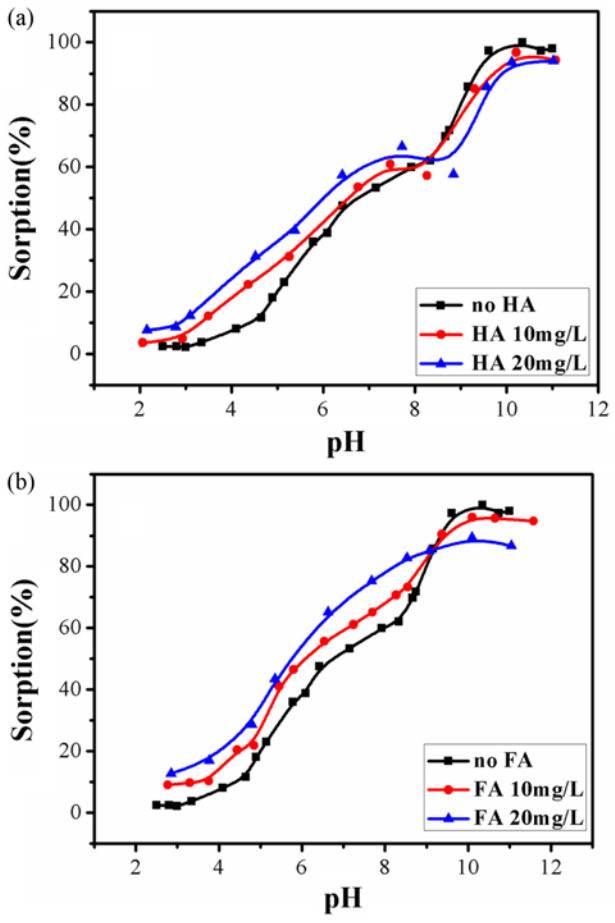

Fig. 13. Effect of HA (a) and FA (b) on Co(II) sorption to SMMWCNTs as a function of pH (T=298.15 K, m/V=0.3 g/L, $C_{[Co(II)]initial}$=0.01 g/L, I=0.01 mol/L NaCl).

curve in NaBr solution is the lowest, and highest in NaF solution. This phenomenon may be attributed to (1) F^- can form complexes with Co(II) in solution, whereas Br^- cannot; (2) Radius order of hydrations is $F^-<Cl^-<Br^-$: the greater radius, the more sorption sites are occupied on SMMWCNTs. This leads to the decrease of Co(II) removal ratio.

As shown in Fig. 12(b), the presence of NO_3^- and ClO_4^- shows no obvious influence on the sorption of Co(II) distinctly. The radical radius order is $ClO_4^->NO_3^->Cl^-$. These negatively charged cations may form complexes or precipitation with functional groups on the surface of SMMWCNTs. But the influence on sorption is still very weak, and this can be interpreted by forming complex on the surface of SMMWCNTs. The influence of ClO_4^-, NO_3^- and Cl^- on the sorption of Co(II) can be ignored.

8. Effect of HA/FA

As two principal components of humic substances, HA and FA can affect the sorption of ions in aqueous solutions. Fig. 13(a) and (b) show the effect of HA and FA on Co(II) sorption to SMMWCNTs. The presence of HA/FA facilitates Co(II) sorption on SMMWCNTs at pH<8, but reduces Co(II) sorption at pH>8. Some researchers [50] determined that HA/FA have negative zeta potentials at pH>2. The increase of Co(II) sorption on SMMWCNTs at low pH value can be attributed to the electrostatic attraction between the negatively charged HA/FA and the acidic SMMWCNTs surface. In consequence, HA/FA enhance Co(II) sorption on SMMWCNTs at pH< 8. With the increase of pH value, the negatively charged HA/FA can no longer attract the negatively charged SMMWCNTs. But HA/FA might combine with Co(II), and thereby reduce sorption of Co(II) on SMMWCNTs at high pH value. The results are in agreement with the Co(II) sorption on multi-walled carbon nanotube-hydroxyapatite composites [51].

9. Sorption Isotherms and Thermodynamic Study

Fig. 14 shows the sorption isotherms of Co(II) on SMMWCNTs at T=298.15 K, 318.15 K and 338.15 K. It is clear that the sorption percentage increases with the temperature rising. To explore the sorption mechanism, the Langmuir and Freundlich isotherm models are used to describe the sorption equilibrium. The Langmuir isotherm is often applicable to a homogeneous sorption surface with all the sorption sites having equal adsorbate affinity. The Langmuir equation can be expressed as follows:

$$q_e=\frac{bq_{e\,max}c_e}{1+bc_e} \tag{6}$$

the line form is:

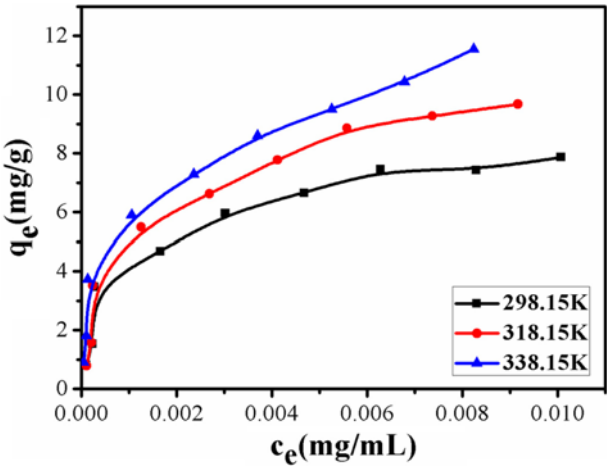

Fig. 14. Sorption isotherms of Co(II) on SMMWCNTs at different temperatures (pH=6.0±0.1, m/V=0.3 g/L, I=0.01 mol/L NaCl).

$$\frac{c_e}{q_e}=\frac{1}{bq_{e\,max}}+\frac{c_e}{q_{e\,max}} \tag{7}$$

where the maximum sorption capacity ($q_{e\,max}$) is the amount of Co(II) at complete monolayer coverage (mg/g), b is the Langmuir constant of equilibrium.

The Freundlich isotherm model is an empirical equation and expressed as follows:

$$q_e=K_F c_e^n \tag{8}$$

After linearization, we obtain:

$$\log q_e=\log K_F+n\log c_e \tag{9}$$

where K_F is the sorption capacity ($mg^{1-n}mL^n/g$); n is the Freundlich constant related to sorption intensity.

Fig. 15(a) and (b) show the fitting results of Langmuir and Freundlich models with the parameters and correlation coefficients (R^2) calculated from corresponding models in Table 3. It is noteworthy that the R^2 calculated by the Langmuir adsorption model is higher, which means the Langmuir adsorption model is more favorable than the Freundlich adsorption model.

Three thermodynamic parameters, the free energy change (ΔG^0) enthalpy change (ΔH^0) and entropy change (ΔS^0) were calculated using the following equations:

$$\Delta G^0=\Delta H^0-T\Delta S^0 \tag{10}$$

$$\ln K_d=\frac{\Delta S^0}{R}-\frac{\Delta H^0}{RT} \tag{11}$$

where R is the gas constant (8.314 J/molK). ΔH^0 and ΔS^0 were calculated from the slope and intercept of Fig. 16 (the plot of $\ln K_d$ versus 1/T). The thermodynamic parameters derived from Eqs. (10)

Table 3. Parameters for Langmuir and Freundlich isotherms at different temperatures

T (K)	Langmuir			Freundlich		
	q_{emax} (mg/g)	b (mL/mg)	R^2	K_F ($mg^{1-n}mL^n/g$)	n	R^2
298.15	8.420	1024	0.993	66.127	0.431	0.864
318.15	10.685	847	0.989	111.923	0.487	0.866
338.15	11.705	1230	0.974	89.875	0.417	0.906

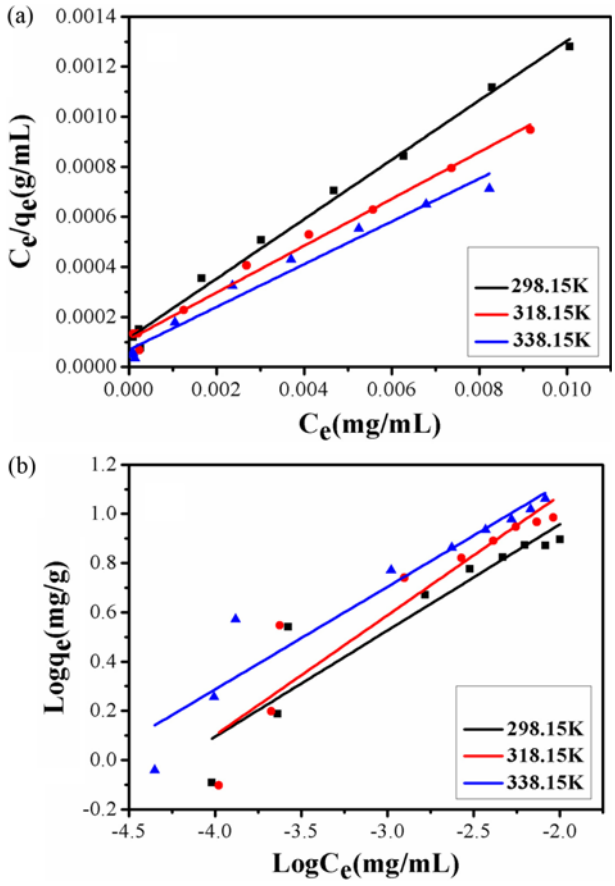

Fig. 15. Langmuir (a) and Freundlich (b) simulation of Co(II) sorption on SMMWCNTs at three different temperatures (pH=6.0±0.1, m/V=0.3 g/L, I=0.01 mol/L NaCl).

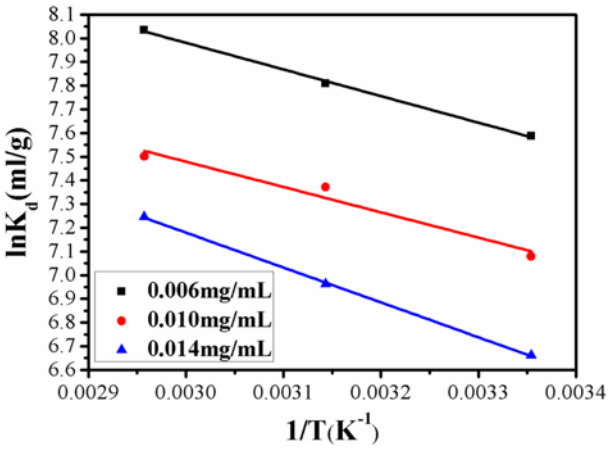

Fig. 16. Effect of temperature on the Co(II) sorption on SMMWCNTs at different initial Co(II) solution concentrations (pH=6.0±0.1, m/V=0.3 g/L, I=0.01 mol/L NaCl).

Table 4. The thermodynamic data of Co(II) sorption on SMMWCNTs at different Co(II) initial solution concentrations

C_0 ($mg \cdot mL^{-1}$)	ΔH^0 ($kJ \cdot mol^{-1}$)	ΔS^0 ($J \cdot mol^{-1} \cdot K^{-1}$)	ΔG^0 ($kJ \cdot mol^{-1}$)		
			298.15 k	318.15 k	338.15 k
0.006	9.346	94.391	−18.797	−20.684	−22.572
0.010	8.890	88.853	−17.601	−19.379	−21.155
0.014	12.124	96.409	−16.504	−18.432	−20.361

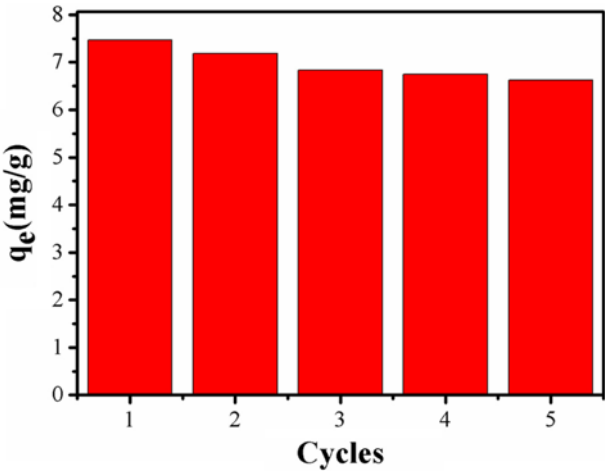

Fig. 17. Recycling of SMMWCNTs on the sorption of Co(II) (T= 298.15 K, pH=6.0±0.1, m/V=0.3 g/L, I=0.01 mol/L NaCl).

and (11) are summarized in Table 4. The positive values of ΔH^0 demonstrate that the sorption is endothermic, which coincides with the sorption isotherms. The value of ΔH^0 is less than 40 $kJ \cdot mol^{-1}$, suggesting that the sorption is a physisorption process. Moreover, the negative values of ΔG^0 indicate that sorption is spontaneous. The decrease of ΔG^0 with an increase of the temperature indicates that sorption is favorable at high temperature. The positive values of ΔS^0 reflect the affinity of adsorbent with Co(II) and imply some structural changes on the adsorbent.

10. Regeneration of Adsorbent

Fig. 17 shows the reuse behavior of SMMWCNTs on Co(II) sorption for a five-cycle test. The results indicate SMMWCNTs bear high sorption capacity of 6.63 mg/g in fifth cycle and 89% retention ratio compared with the first cycle. Therefore, the SMMWCNTs can be a good reusable adsorbent for the sorption of Co(II) from large volumes of aqueous solutions.

CONCLUSION

Sulfonated magnetic multi-walled carbon nanotubes were successfully synthesized through an environmentally friendly process. SMMWCNTs display high stability in aqueous solutions and can be well dispersed in water for 12 h. SMMWCNTs also exhibit an excellent magnetic property, meaning a good dispersion and easy separation during the wastewater treatment.

Batch sorption tests demonstrate that the sorption is affected by various conditions, such as solution pH, ionic strength, contact time, cations, anions, HA/FA and temperature. The sorption of Co(II) is a fast process, and the pseudo-second-order model could fit the data much better than the pseudo-first-order. Foreign anions (F^- and Br^-) exhibit obvious influence on sorption, while cations (Mg^{2+} and Ca^{2+}) restrain sorption strongly. The existence of HA/FA enhances sorption process at pH<8, while weakens at pH>8. The Langmuir adsorption model is more favorable than the Freundlich adsorption model. Thermodynamic studies reveal that the sorption process is endothermic and spontaneous. The regeneration test determines that SMMWCNTs can be used repeatedly for the sorption of Co(II) from aqueous solutions. Thus, this SMMWCNT sorbent is believed to be a promising material for the selective removal of Co(II) from heavy metal-containing wastewater.

ACKNOWLEDGEMENT

This study was supported by the Project of Shandong Province Higher Educational Science and Technology Program (No. J14LC09). All of the authors express their deep thanks.

REFERENCES

1. X. Xin, Q. Wei, J. Yang, L. Yan, R. Feng, G. Chen, B. Du and H. Li, *Chem. Eng. J.*, **184**, 132 (2012).
2. Y. Zhang, L. Yan, W. Xu, X. Guo, L. Cui, L. Gao, Q. Wei and B. Du, *J. Mol. Liq.*, **191**, 177 (2014).
3. G. Klug, *Mol. Microbiol.*, **91**, 635 (2014).
4. F. Fang, L. Kong, J. Huang, S. Wu, K. Zhang, X. Wang, B. Sun, Z. Jin, J. Wang, X. J. Huang and J. Liu, *J. Hazard. Mater.*, **270**, 1 (2014).
5. G. S. Kamble, A. A. Ghare, S. S. Kolekar, S. H. Han and M. A. Anuse, *Spectrochim. Acta A*, **84**, 117 (2011).
6. D. Manohar, B. Noeline and T. Anirudhan, *Appl. Clay. Sci.*, **31**, 194 (2006).
7. J. M. Diamond, E. L. Winchester, D. G. Mackler, W. J. Rasnake, J. K. Fanelli and D. Gruber, *Aquat. Toxicol.*, **22**, 163 (1992).
8. Q. Chang and G. Wang, *Chem. Eng. Sci.*, **62**, 4636 (2007).
9. X. T. Le, P. Viel, A. Sorin, P. Jegou and S. Palacin, *Electrochim. Acta*, **54**, 6089 (2009).
10. L. G. Yan, Y. Y. Xu, H. Q. Yu, X. D. Xin, Q. Wei and B. Du, *J. Hazard. Mater.*, **179**, 244 (2010).
11. X. Guo, Q. Wei, B. Du, Y. Zhang, X. Xin, L. Yan and H. Yu, *Appl. Surf. Sci.*, **284**, 862 (2013).
12. X. Xin, W. Si, Z. Yao, R. Feng, B. Du, L. Yan and Q. Wei, *J. Colloid Interface Sci.*, **359**, 499 (2011).
13. F. L. Fu and Q. Wang, *J. Environ. Manage.*, **92**, 407 (2011).
14. B. Alyüz and S. Veli, *J. Hazard. Mater.*, **167**, 482 (2009).
15. D. Mohan and K. P. Singh, *Water Res.*, **36**, 2304 (2002).
16. Y.-H. Li, S. Wang, Z. Luan, J. Ding, C. Xu and D. Wu, *Carbon*, **41**, 1057 (2003).
17. M. Machida, T. Mochimaru and H. Tatsumoto, *Carbon*, **44**, 2681 (2006).
18. Z. Liu, L. Chen, Y. Dong and Z. Zhang, *J. Radioanal. Nucl. Chem.*, **289**, 851 (2011).
19. X. Tang, Q. Zhang, Z. Liu, K. Pan, Y. Dong and Y. Li, *J. Mol. Liq.*, **191**, 73 (2014).

20. M. Harja, G. Buema, D. M. Sutiman, C. Munteanu and D. Bucur, *Korean J. Chem. Eng.*, **29**, 1735 (2012).
21. L. Panda, B. Das and D. S. Rao, *Korean J. Chem. Eng.*, **28**, 2024 (2011).
22. R. Lafi, A. Fradj, A. Hafiane and B. H. Hameed, *Korean J. Chem. Eng.*, **31**, 2198 (2014).
23. S. H. Khorzughy, T. Eslamkish, F. D. Ardejani and M. R. Heydartaemeh, *Korean J. Chem. Eng.*, **32**, 88 (2015).
24. P. S. Kumar, S. Ramalingam, V. Sathyaselvabala, S. D. Kirupha, A. Murugesan and S. Sivanesan, *Korean J. Chem. Eng.*, **29**, 756 (2012).
25. I. Lee, J. A. Park, J. K. Kang, J. H. Kim, J. W. Son, I. G. Yi and S. B. Kim, *Environ. Eng. Res.*, **19**, 157 (2014).
26. S. Iijima, *Nature*, **354**, 56 (1991).
27. F. N. Behdani, A. T. Rafsanjani, M. Torab-Mostaedi and S. M. A. K. Mohammadpour, *Korean J. Chem. Eng.*, **30**, 448 (2013).
28. N. M. Mubarak, R. K. Thines, N. R. Sajuni, E. C. Abdullah, J. N. Sahu, P. Ganesan and N. S. Jayakumar, *Korean J. Chem. Eng.*, **31**, 1582 (2014).
29. N. Sankararamakrishnan, M. Jaiswal and N. Verma, *Chem. Eng. J.*, **235**, 1 (2014).
30. M. A. Tofighy and T. Mohammadi, *Korean J. Chem. Eng.*, **32**, 292 (2015).
31. P. Xu, G. M. Zeng, D. L. Huang, C. L. Feng, S. Hu, M. H. Zhao, C. Lai, Z. Wei, C. Huang, G. X. Xie and Z. F. Liu, *Sci. Total Environ.*, **424**, 1 (2012).
32. N. M. Mubarak, J. N. Sahu, E. C. Abdullah and N. S. Jayakumar, *Sep. Purif. Rev.*, **43**, 311 (2014).
33. M. Farbod, S. K. Tadavani and A. Kiasat, *Colloids Surf., A*, **384**, 685 (2011).
34. Y. Ge, Z. Li, D. Xiao, P. Xiong and N. Ye, *J. Ind. Eng. Chem.*, **20**, 1765 (2013).
35. X. Tan, M. Fang, C. Chen, S. Yu and X. Wang, *Carbon*, **46**, 1741 (2008).
36. X. Xie, L. Gao and J. Sun, *Colloids Surf., A*, **308**, 54 (2007).
37. P. R. Chang, P. Zheng, B. Liu, D. P. Anderson, J. Yu and X. Ma, *J. Hazard. Mater.*, **186**, 2144 (2011).
38. S. Yang, J. Li, Y. Lu, Y. Chen and X. Wang, *Appl. Radiat. Isot.*, **67**, 1600 (2009).
39. X. Ren, D. Shao, S. Yang, J. Hu, G. Sheng, X. Tan and X. Wang, *Chem. Eng. J.*, **170**, 170 (2011).
40. H. Cao, M. Zhu, Y. Li, J. Liu, Z. Ni and Z. Qin, *J. Solid State Chem.*, **180**, 3218 (2007).
41. Y. Shan and L. Gao, *Nanotechnology*, **16**, 625 (2005).
42. Y. Ge, Z. Li, D. Xiao, P. Xiong and N. Ye, *J. Ind. Eng. Chem.*, **20**, 1765 (2014).
43. A. K. Mishra and S. Ramaprabhu, *J. Phys. Chem. C*, **114**, 2583 (2010).
44. B. Jia and L. Gao, *J. Phys. Chem. B*, **111**, 5337 (2007).
45. F. Yu, J. Chen, L. Chen, J. Huai, W. Gong, Z. Yuan, J. Wang and J. Ma, *J. Colloid Interface Sci.*, **378**, 175 (2012).
46. T. Madrakian, A. Afkhami, M. Ahmadi and H. Bagheri, *J. Hazard. Mater.*, **196**, 109 (2011).
47. W. H. Cheung, Y. S. Szeto and G. McKay, *Bioresour. Technol.*, **98**, 2897 (2007).
48. R. D. Harter and R. Naidu, *Soil. Sci. Soc. Am. J.*, **65**, 597 (2001).
49. F. Esmadi and J. Simm, *Colloids Surf., A*, **104**, 265 (1995).
50. X. Tan, X. Wang, H. Geckeis and T. Rabung, *Environ. Sci. Technol.*, **42**, 6532 (2008).
51. Z. Liu, L. Chen, Z. Zhang, Y. Li, Y. Dong and Y. Sun, *J. Mol. Liq.*, **179**, 46 (2013).